Karlsruhe Institute of Technology (KIT)
Institute for Neutron Physics and Reactor Technology (INR)
Fusion Neutronics Group
Hermann-von-Helmholtz-Platz 1
D-76344 Eggenstein-Leopoldshafen
http://www.inr.kit.edu

TRANSMUTATION EFFECTS IN MATERIALS FOR ITER DIAGNOSTICS

Arkady Serikov[a], Luciano Bertalot[b], Ulrich Fischer[a], Dieter Leichtle[a]

[a]*Karlsruhe Institute of Technology KIT, Institute for Neutron Physics and Reactor Technology, Hermann-von-Helmholtz-Platz 1, 76344 Eggenstein-Leopoldshafen, Germany*
[b]*ITER Organization, Route de Vinon sur Verdon, 13115 Saint Paul Lez Durance, France*

Thermocouples due to Transmutation of Cu and Au in Cable Looms

- The cable looms are distributed all around the ITER and attached to the inner wall of the Vacuum Vessel (VV) and under the divertor cassettes.
- The results include distributions of neutronics characteristics calculated with the MCNP5 3D Monte Carlo code assuming ITER operation with 0.54 Full Power Years (FPY) on 500 MW fusion power of DT plasma with 14 MeV neutron source defined in the modified MCNP B-lite model of ITER tokamak.

Two hot spots at the entrance to Upper Port

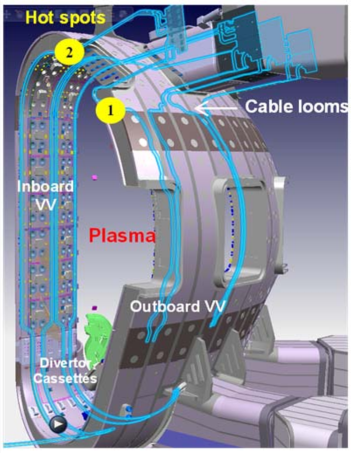

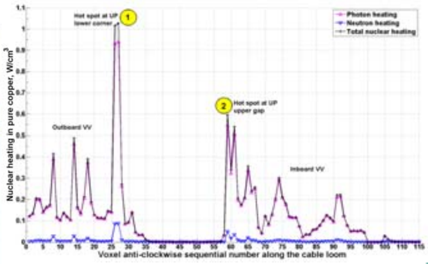

- **The major transmutation of gold and copper** is observed on the (n,g) radiative capture reactions.
- **The maximum transmutation** was observed in gold, amounted 3 atom% for the highest radiation spot at the in-vessel loom, and 1 atom% for the divertor cassette.
- **Transmutation of copper is 100 times less than gold**; it is 0.03 atom% for the hot-spot at divertor and 0.01 atom% for in-vessel loom.

$^{65}Cu(n,\gamma)^{66}Cu$ ($T_{1/2}$ = 5 min, beta decay)--> ^{66}Zn

$^{63}Cu(n,\gamma)^{64}Cu$ ($T_{1/2}$ = 12.7 h, positron decay)--> ^{64}Ni

$^{197}Au(n,\gamma)\,^{198}Au \rightarrow \,^{198}Hg + \beta^-$ ($T_{1/2}$ = 2.7 days, beta decay)

Table 1: Gold transmutation used in cable looms

Voxel number at peak of radiation	Reaction of transmutation	Au transmutation, appm/0.54 FPY	Relative stat. error of Au transmut. reaction
Voxel #6 on loom of divertor side	total (n,p)	3.86E-02	4.55E-02
	total (n,He)	5.78E-03	4.61E-02
	(n,g)	1.33E+04	8.98E-02
Voxel #17 on loom of divertor side	total (n,p)	2.49E-02	5.69E-02
	total (n,He)	3.77E-03	5.77E-02
	(n,g)	1.12E+04	1.35E-01
Voxel #27 on in-vessel loom	total (n,p)	7.43E-02	2.99E-02
	total (n,He)	1.10E-02	3.04E-02
	(n,g)	2.97E+04	1.04E-01
Voxel #59 on in-vessel loom	total (n,p)	4.16E-02	4.15E-02
	total (n,He)	6.19E-03	4.21E-02
	(n,g)	1.49E+04	1.45E-01

Table 2: Transmutation: $^{63}Cu \rightarrow {}^{64}Ni$ and $^{65}Cu \rightarrow {}^{66}Zn$

Voxel number at peak	Reaction of transmutation	^{63}Cu transmutation, appm/0.54 FPY	^{65}Cu transmutation, appm/0.54 FPY
Voxel #6 on loom of divertor side	total (n,p)	8.10E+00	9.28E-01
	total (n,He)	1.27E+00	2.29E-01
	(n,g)	3.66E+02	1.76E+02
Voxel #17 on loom of divertor side	total (n,p)	5.57E+00	6.12E-01
	total (n,He)	8.44E-01	1.49E-01
	(n,g)	2.67E+02	1.28E+02
Voxel #27 on in-vessel loom	total (n,p)	1.54E+01	1.75E+00
	total (n,He)	2.38E+00	4.38E-01
	(n,g)	1.67E+02	9.07E+01
Voxel #59 on in-vessel loom	total (n,p)	8.41E+00	9.74E-01
	total (n,He)	1.32E+00	2.45E-01
	(n,g)	1.20E+02	4.07E+01

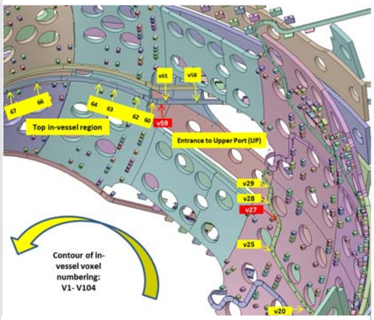

Voxels along the in-vessel loom with max loads at the entrance to Upper Port (v27) and Top in-vessel (v59)

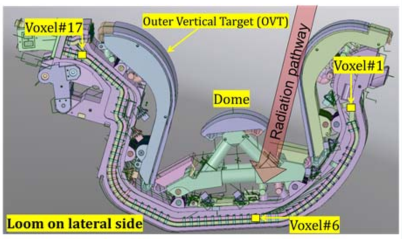

Vertical cut of the CAD model of the divertor cassette with the cable loom at its lateral side

Use of gold (Au) in connectors for diagnostics at inboard blanket

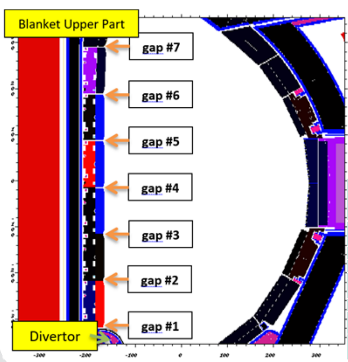

Transmutation of gold inside the inter-blanket gaps of inboard blanket between its FW and beginning of VV.

Conclusions for gold transmutation:
- Highest cross-section is (n,g) producing mercury through beta-decay of **Au-198**.
- Other transmutation reactions such as (n,p), (n,d), (n,t), (n,alpha) with production of **Pt, Ir** have much lower (lower by 4-5 orders of magnitude) cross-sections.

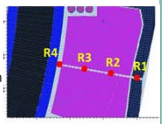

Horizontal Gap Nr.	Z, cm	R1 =406.8 cm at FW, appm/0.54 FPY	R2=389.8 cm, appm/0.54 FPY	R3=372.8 cm, appm/0.54 FPY	R4=356.8 cm at VV, appm/0.54 FPY
Upper level 7	357.50	1.02E+05	3.60E+04	1.09E+04	3.69E+03
6	255.50	1.14E+05	5.91E+04	2.16E+04	8.30E+03
5	154.50	1.16E+05	6.70E+04	3.09E+04	1.02E+04
Middle level 4	52.50	1.19E+05	7.56E+04	3.04E+04	1.25E+04
3	-48.50	1.13E+05	6.09E+04	2.83E+04	1.26E+04
2	-150.50	1.01E+05	6.30E+04	2.00E+04	9.80E+03
Lower level 1	-253.50	8.42E+04	4.34E+04	1.25E+04	6.38E+03

Dominance of Decay Heat in Transmuted Rhodium of CXRS mirrors

CXRS-Core in Upper Port Plug (UPP) #3

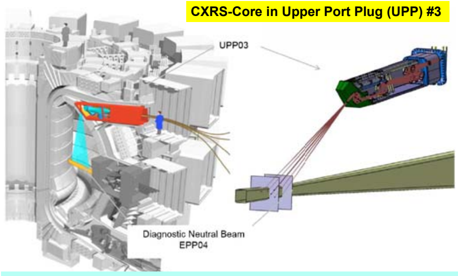

Actual MCNP C-Model of ITER tokamak

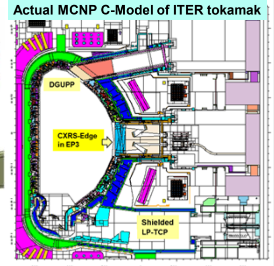

Neutronics MCNP model and an underlying CAD model of CXRS-Core in UP3 (design is progressing)

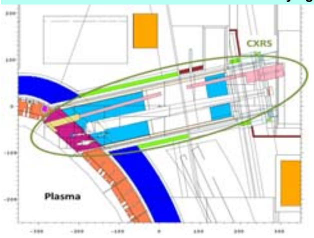

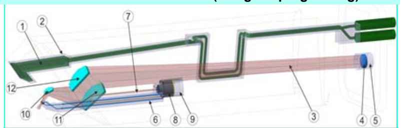

1. GDC Antenna
2. GDC Antenna cutout volume
3. Optical path cutout volume
4. Window
5. Window cutout at the closure plate
6. Shutter components
7. Shutter cutout volume
8. Actuator
9. Actuator cutout volume
10. M1
11. M2
12. M3

Natural Rhodium consists of a single isotope Rh-103. During ITER irradiation, it transmutes by neutron capture to Rh-104. This isotope is instable and undergoes beta decay (**half-life 42.3 s**) to stable Palladium-104. The maximum beta energy is 2.44 MeV with its average of 0.995 MeV.

Comparison decay vs. prompt heat in Rh: Decay heat in transmuted Rh dominates its nuclear heating

Prompt heat in potential materials of M1

Material	Density [g/cm³]	Prompt (neutron+photon) heat [W/cm³]
80% W, 20% Cu	15.00	3.85
Rhodium	12.41	1.24
Molybdenum	10.29	1.64
Inconel 718	8.20	1.29
SS316L(N)-IG	7.93	1.12
Aluminium Bronze	7.60	1.12
Ti-6Al-4V	4.41	0.618
Aluminum nitride	3.26	0.603
RSA-905 alloy	2.95	0.463
Aluminium	2.70	0.425

Decay heat in transmuted Rhodium of M1

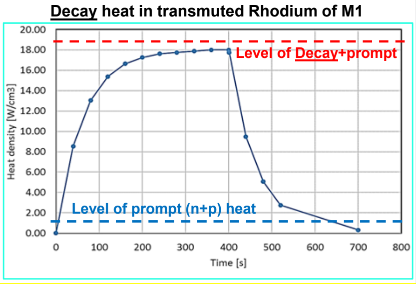

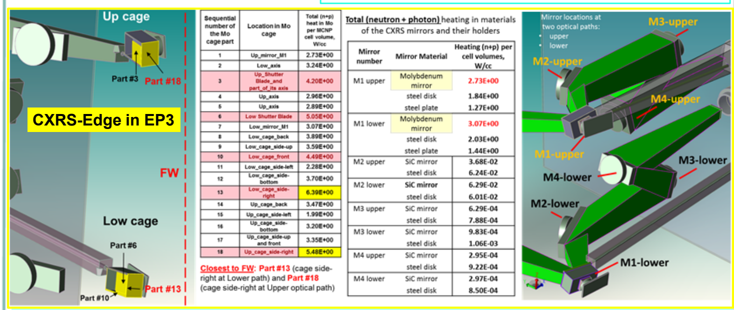

Conclusions and recommendation for nuclear heat calculation in Rhodium (Rh)

- The temperature gradients together with the nuclear transmutation of the cable's copper [1] could result in formation of thermocouples and hence non-inductive parasitic voltages due the Radiation-Induced Thermoelectric Sensitivity (RITES) effect [2]. This transmutation effect should be reduced in order to enhance the performance of the magnetic sensors.
- Case of M1 in front of CXRS on hard spectrum demonstrated 20 times higher decay heat than prompt (neutron + photon) heat in Rh. It indicates mandatory of Rh activation calculations in its nuclear heating assessments. Other studied mirror materials show negligible decay heat contribution.
- In other cases of using Rh under neutron irradiation, the factor of decay heat dominance could be even higher because radioactive isotope Rh-104 is produced on (n,g) reaction which is reversed proportional to neutron energy, and (n,g) is higher on softer spectra.
- Decay heat during a 400 s plasma pulse raises quickly and saturates at 18 W/cc. Due to the short half-life of 42.3 s, it decays rapidly after the pulse.

References

[1] A. Serikov, et al., Neutronics analysis for ITER cable looms, Fusion Engineering and Design, 96–97 (2015) 943–947.
[2] G. Vayakis, et al., Radiation-induced thermoelectric sensitivity (RITES) in ITER prototype magnetic sensors, Review of Scientific Instruments, 75 (2004) 4324-4327.

Acknowledgments & Disclaimer

This work has been partly funded by the ITER Organization (IO) under the ITER service contract No. IO/17/CT/4300001748 and by the Fusion for Energy (F4E) Specific Grant FPA-408-SG04. This work was carried out using the adaptions of the B-lite model and C-model which were developed as a collaborative effort between: AMEC Co (International), CCFE (UK), ENEA Frascati (Italy), FDS Team of INEST (PRC), ITER Organization (France), QST (Japan), KIT (Germany), UNED (Spain), University of Wisconsin-Madison (USA), F4E (Europe).
The views and opinions expressed herein do not necessarily reflect those of the ITER Organization. This paper does not commit the IO as a nuclear operator.

*Corresponding author: arkady.serikov@kit.edu